A Theoretical Study of the CH_2N System: Reactions in both Lowest Lying Doublet and Quartet States

Raman Sumathi and Minh Tho Nguyen*

Department of Chemistry, University of Leuven, Celestijnenlaan 200F, B-3001 Leuven, Belgium

Received: March 18, 1998; In Final Form: June 3, 1998

Ab initio molecular orbital calculations at the second-order perturbation theory (UMP2) and coupled cluster singles and doubles with corrected triples (CCSD(T)) levels with 6-311++G(d,p) and 6-311++G(3df,3dp) basis sets have been carried out to construct the potential energy surfaces related to the various reactions of the $[CH_2N]$ system, including H_2+CN, H+HCN, and H+HNC in both lowest lying doublet and quartet electronic states. Barrier heights, vibrational wavenumbers, and moments of inertia were then utilized in the calculations of rate constants using a quantum Rice−Ramsperger−Kassel (QRRK) theory. The calculated total rate constant k_∞ for the H+HCN reaction at 300 K is 2.2×10^7 cm^3 mol^{-1} s^{-1} and is suggestive of a slow reaction and it corresponds predominantly to the stabilization of the adducts. On the other hand, the H+HNC reaction is calculated to be a pressure-independent fast reaction with a rate coefficient of 1.9×10^{11} cm^3 mol^{-1} s^{-1} leading primarily to H+HCN dissociation products. The standard heat of formation of the H_2CN radical is estimated to be $\Delta H^0_{f,298} = 56 \pm 3$ kcal/mol (57 ± 3 kcal/mol at 0 K).

1. Introduction

The $[CH_2N]$ isomeric system is of wide interest. In the combustion and atmospheric chemistry, the reaction i

$$H_2 + CN \rightarrow HCN + H \qquad \text{(i)}$$

is shown to be an important elementary step in the formation of NO pollutants from atmospheric nitrogen and nitrogen-containing fuels,[1] as well as an important step in the flame processes of nitramine propellants.[2] There have been several measurements of the rate constant for the forward reaction, both at high[3] and low temperatures.[4−6] In addition, the forward reaction has been studied at room temperature as a function of initial vibrational excitation[6] and its dynamics has also been investigated in detail by a collinear reactive scattering and quasiclassical trajectory calculations.[7] However, the reverse reaction has never been studied experimentally for it is highly endothermic. The C−H bond in HCN is quite strong, the associated bond energy being about 124 kcal/mol. Consequently, in the isolated HCN molecule, the dissociation pathway is unimportant, and in fact, its isomerization to HNC is the only predominant channel. This isomerization has been shown to have a barrier of about 47.5 kcal/mole,[8] and it provides a facile unimolecular reaction pathway for the relatively stable HCN moiety. Lin et al.[9] reported a computed rate constant ($3.5 \times 10^{13} \exp(-23750/T)$ s^{-1}) for this isomerisation. In presence of the hydrogen atom, one would expect that addition to the triple bond would be more important than abstraction. The addition product would then undergo further isomerizations and dissociation to yield HNC+H. Hence, it is of interest to study the conversion of HCN to HNC in presence of hydrogen and to compare them with the isomerization of the isolated HCN molecule.

The current conventional wisdom also assumes that the $[CH_2N]$ species are, along with their $(CH_2N)^+$ ions, the potential precursors of both HCN and HNC in the interstellar cloud[10] via reactions ii and iii.

$$H_2C + N \rightarrow HCN + H \qquad \text{(ii)}$$

$$H_2C + N \rightarrow HNC + H \qquad \text{(iii)}$$

Although these reactions have been repeatedly put forward, to our knowledge, they have not been studied experimentally yet. While the H_2CN radical is formed upon gas phase decomposition of several imine and azoalkane compounds, the iminomethyl (HCNH) and aminocarbyne (CNH_2) isomers are also believed to be intermediates in the thermal decomposition of methylamine and azomethane and hydrogenation of HCN on various metal surfaces[11] (Si, Ni, Ru, Pt, etc.).

Interest in these different fields indicates that there is much to be gained by the construction of reliable potential energy surface (PES) of the $[CH_2N]$ system covering most, if not all, of the transformations and interconnections of the corresponding isomers. Up to now, theoretical studies have mainly been focused on the properties of H_2CN, the most stable isomer[12] and on the hydrogen abstraction reaction i.[13,14] A significant contribution has been made by Bair et al.[13,14] with a GVB-CI treatment towards the understanding of the lowest-lying doublet potential energy surface of $[CH_2N]$, though containing only three of its isomers, viz., H_2CN, *cis*-HCNH, and *trans*-HCNH. They then determined the ab initio rate constant for the direct hydrogen abstraction reaction i using the conventional transition state theory. Recently, we have reported[15] a more complete PES of the lowest lying doublet electronic state, including the pathways linking five equilibrium structures, namely, H+HCN, H+HNC, H_2CN, HCNH, and CNH_2. The purpose of our earlier study, whose results were obtained using quadratic configuration interaction QCISD(T)/6-311++G(3df,2p) calculations, was to probe the participation of the $[CH_2N]$ isomers during decomposition of methyl azide and methanimine. Hence, the reactions i, −i, ii, and iii were not considered and details of the calculated

* To whom correspondence should be addressed. Fax: 32-16-327992. E-mail: minh.nguyen@chem.kuleuven.ac.be.

S1089-5639(98)01542-4 CCC: $15.00
Published on Web 09/19/1998

structures and energetics have not been reported in ref 15. More importantly, perhaps, is the fact that both reactions ii and iii are not likely to occur in the ground doublet electronic state. The preliminary experiment[16] on reaction iii between the triplet methylene and atomic nitrogen using the discharge flow-molecular beam mass spectrometric techniques (DF-MBMS) indicated that HCN has been produced in its triplet state rather than in its singlet ground state. This implies that this reaction is likely to proceed through an excited doublet or quartet state of the $[CH_2N]$ system.

In an attempt to map out a reliable and uniform potential energy surface including most of the possible reaction channels mentioned above of the $[CH_2N]$ species and as a preliminary step for the subsequent kinetic analysis, we have carried out high-level ab initio molecular orbital calculations in both lowest lying doublet and quartet electronic states. Calculations on an excited doublet state have been abandoned by a practical reason that, for the structures having no symmetry, this state cannot be constructed using the unrestricted Hartree−Fock (UHF) based single-reference method that we have adopted for the present work. It is well-known that, in these cases, only the wave functions corresponding to the lowest lying electronic state could be characterized.

After mapping out the energy surfaces, we have then utilized the computed thermochemical, vibrational, and rotational parameters of the stationary points as inputs for calculating the individual and total rate constants of H+HCN and H+HNC reactions within the framework of a QRRK theory.[17] The kinetic analyses allow the possibility of formation of each isomer and the competition between various reaction channels to be established. It is needless to say that, even though the QRRK formalism is less rigorous than the Rice−Ramsperger−Kassel−Marcus (RRKM) approach, the overall reaction mechanism can be extracted from this simple treatment. Concerning the values of rate constants, both treatments give overall comparable values as they are mainly determined by geometrical and energetic parameters. The main advantage of the QRRK treatment lies in the fact that it is easy to implement for chemically activated reactions containing several energized intermediates and multiple channels.

2. Method of Calculation

Ab initio molecular orbital calculations were carried out using the Gaussian 94 set of programs.[18] The open shell calculations were performed using the unrestricted Hartree−Fock formalism. The potential energy surface was initially mapped out using UMP2 calculations in conjunction with the 6-31G(d,p) basis set. Stationary points were then characterized by harmonic vibrational frequency analyses at this level. The identity of each first-order stationary point is determined when necessary, by intrinsic reaction coordinate (IRC) calculations. Geometries of the relevant equilibrium and transition structures were then reoptimized using the coupled-cluster method including all single and double excitations plus a perturbative estimation of the contributions of the connected triple substitutions to the correlation energy with the same basis set, CCSD(T)/6-311++G(d,p). Improved energies of all stationary points were further estimated using single-point electronic energy CCSD(T) calculations at the CCSD(T) geometries with the larger 6-311++G(3df,3pd) one-electron basis set. In the coupled-cluster calculations, only the valence electrons are included in the correlation procedure. The zero-point energies were derived from harmonic vibrational wavenumbers at the UMP2/6-31G(d,p) level and scaled down by a uniform factor of 0.94. Throughout this paper, bond lengths are given in angströms, bond angles in degrees, zero-point and relative energies in kcal/mol, unless otherwise stated.

TABLE 1: Calculated CCSD(T)/6-311++G(3df,3pd) Total Energies in Atomic Units and ZPE in kcal/mol for Species Involved in the $[H_2CN]$ PES

species	total energy[a]	ZPE[b]
H_2CN, **1**	−93.8241 10	17.2
t-HCNH, **2**	−93.8117 94	17.6
c-HCNH, **3**	−93.8036 62	16.9
CNH_2, **4**	−93.7773 53	17.2
1/**2**	−93.7473 03	14.1
2/**3**	−93.7848 26	16.3
2/**4**	−93.7104 79	12.6
1/**6**	−93.7656 60	12.5
3/**7**	−93.7480 59	10.5
3/**6**	−93.7598 15	12.2
4/**7**	−93.7311 74	11.8
5/**6**	−93.7320 43	11.4
1q	−93.6833 22	15.5
2q	−93.6597 79	15.2
4q	−93.6464 27	17.4
1q/**2q**	−93.6032 27	12.4
2q/**4q**	−93.5818 07	13.5
1q/**6q**	−93.5949 92	9.9
2q/**6q**	−93.5921 49	10.1
2q/**7q**	−93.5753 77	10.4
4q/**7q**	−93.5748 12	10.6

[a] Based on optimized geometries at the CCSD(T)/6-311++G(d,p) level. [b] Zero-point energies using unscaled frequencies at UMP2/6-31G(d,p) level.

3. Results and Discussion

Calculated total energy and zero-point vibrational energies of the species examined are tabulated in Table 1. Let us first describe briefly the essential features of the lowest-lying doublet and quartet PES's related to the $[CH_2N]$ system schematically shown in Figure 1. Each stationary point in Figure 1 is labeled with a number in order to facilitate the discussion. While the equilibrium positions are associated with the numbers from **1** to **9**, the transition structures (TS) are defined by **X**/**Y** where **X** and **Y** are the two connected equilibrium structures. As can be seen, the PES consists of four isomers, namely H_2CN **1**, trans-HCNH, **2**, cis-HCNH, **3**, and CNH_2, **4**, and the different first-order saddle points connecting these minima to different product limits, viz., H_2 + CN, **5**; H+HCN, **6**; H+HNC, **7**; C+NH_2, **8**, and N+CH_2, **9**. The CCSD(T)/6-311++G(d,p) optimized geometries of the TSs **1**/**2**, **2**/**3**, **2**/**4**, **1**/**6**, **3**/**6**, **3**/**7**, **4**/**7** and also the direct hydrogen abstraction TS **5**/**6** on the doublet potential energy surface are shown in Figure 2, while the corresponding stationary points on the quartet PES are shown in Figure 3. The numbers in parentheses in Figures 2 and 3 correspond to UMP2/6-31G(d,p) level of optimization. The CCSD(T)/6-311++G(3df,3pd)//CCSD(T)/6-311++G(d,p) energies are shown in Figure 1 relative to that of the H_2CN limit **1** with appropriate zero-point vibrational energy corrections using UMP2 frequencies. The values given in parantheses represent the GVB-CI results obtained by Bair and Dunning.[13] The most important result is perhaps the fact that both the doublet and quartet PESs are well separated from each other. The highest lying doublet transition state TS **2**/**4** is about 20 kcal/mol below the lowest lying quartet structure H_2CN, **4q**. The unscaled harmonic vibrational frequencies of the various stationary points on the

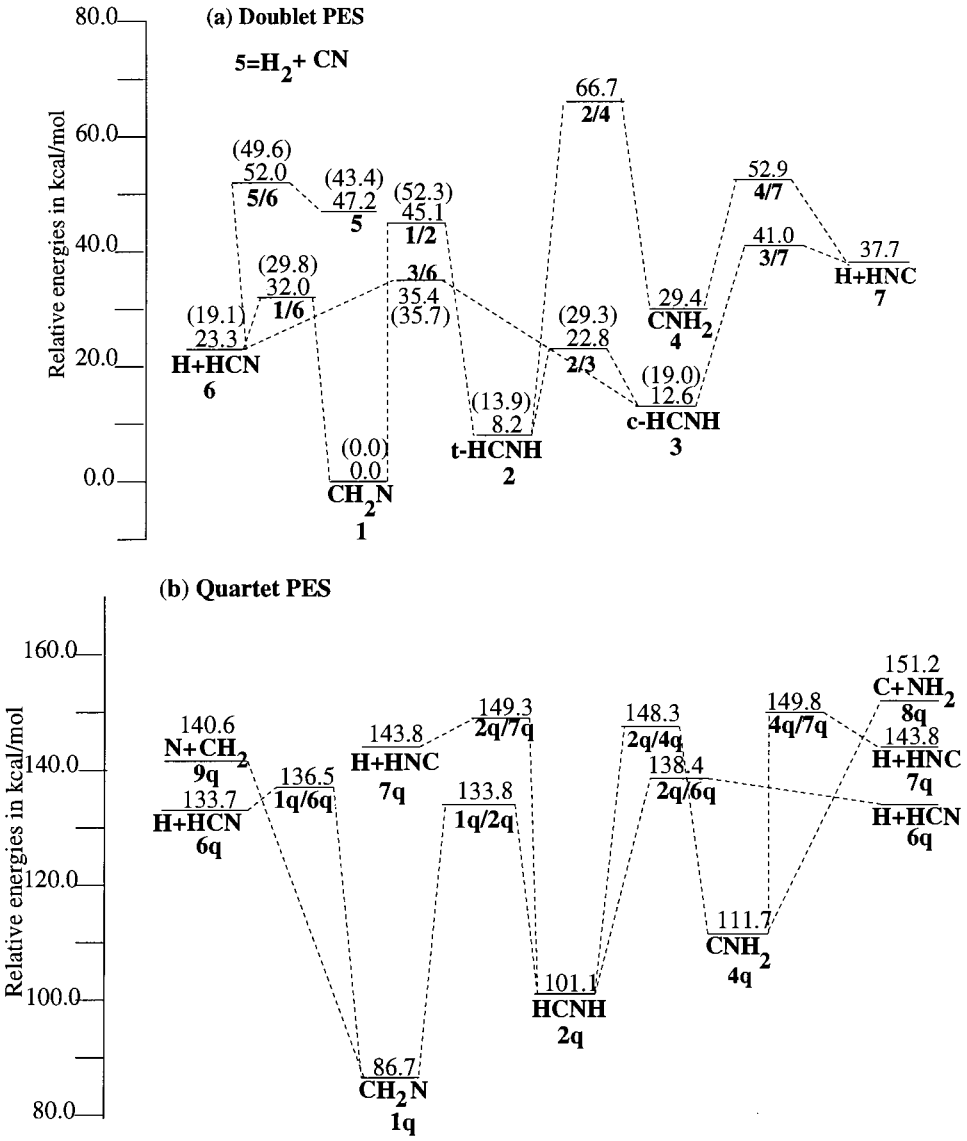

Figure 1. The overall profile of the (a) doublet and (b) quartet PES for the [CH_2N] system calculated at CCSD(T)/6-311++G(3df,3pd) //CCSD-(T)/6-311++G(d,p) +ZPE level of theory. Values in parentheses in (a) correspond to the POL-CI ones taken from ref 13. In the quartet PES, HCN, and HNC correspond to the triplet $^3A''$ state.

doublet and quartet PES's are tabulated respectively, in Tables 2 and 3 and are available as Supporting Information.

Energetically, H_2CN, **1**, was found to be more stable than trans-HCNH, **2** by 8.2 kcal/mol. The 1,2-hydrogen shifts from carbon to nitrogen, and the reverse occur from the trans isomer with the latter being energetically favored over the former migration. The calculated three-membered TSs including the migrating hydrogen, the origin and the terminus centers of migration, **1**/**2** and **2**/**4**, for these shifts have the hydrogens in a trans relationship. In addition to these 1,2-hydrogen shifts, **2** can undergo cis−trans isomerization leading to the higher energy cis conformer **3** via **2**/**3**. The two possible unimolecular dissociation pathways of HCNH, namely, dissociation into HCN+H, **6**, and HNC+H, **7**, proceed only from the higher energy cis-conformer. The dissociation of C−H and N−H bonds in **3** involve barriers of 32.8 and 27.2 kcal/mol, respectively, and are, therefore, relatively difficult compared to the cis-trans isomerisation of **3**. The barrier for the hydrogen attack at the C-center of HCN, H+HCN, **6** → H_2CN, **1**, was calculated to be 8.7 kcal/mol and this value is in close agreement with our earlier QCISD(T)/6-311++G(3df,2p) results (7.3 kcal/mol)[15] but differs somewhat from the value of 10.7 kcal/mol reported by Bair et al.[13] for the same process using POL-CI calculations. In addition to this attack, the addition could take place to the nitrogen end of HCN giving rise to *cis*-HCNH. As discussed by Bair et al. the saddle point for the H addition to the nitrogen does not lead to the most stable isomer of HCNH, viz., trans-HCNH, **2**, but rather to *cis*-HCNH, **3**. This is presumably due to a stereoelectronic effect such as in the case of the HNC+H^- addition.[19] Though, the initial barrier for hydrogen attack at the nitrogen site of HCN is slightly higher (12.1 kcal/mol) than that at the carbon site (8.7 kcal/mol), the saddle point for cis−trans isomerization, **2**/**3**, lies energetically below **3**/**6**. The various pathways starting from H+HCN, **6**, leading to H+HNC are

H + HCN **6** → **1** → **2** → **3** → H + HNC **7** (A)

H + HCN **6** → **1** → **2** → **4** → H + HNC **7** (B)

H + HCN **6** → **3** → H + HNC **7** (C)

H + HCN **6** → **3** → **2** → **4** → H + HNC **7** (D)

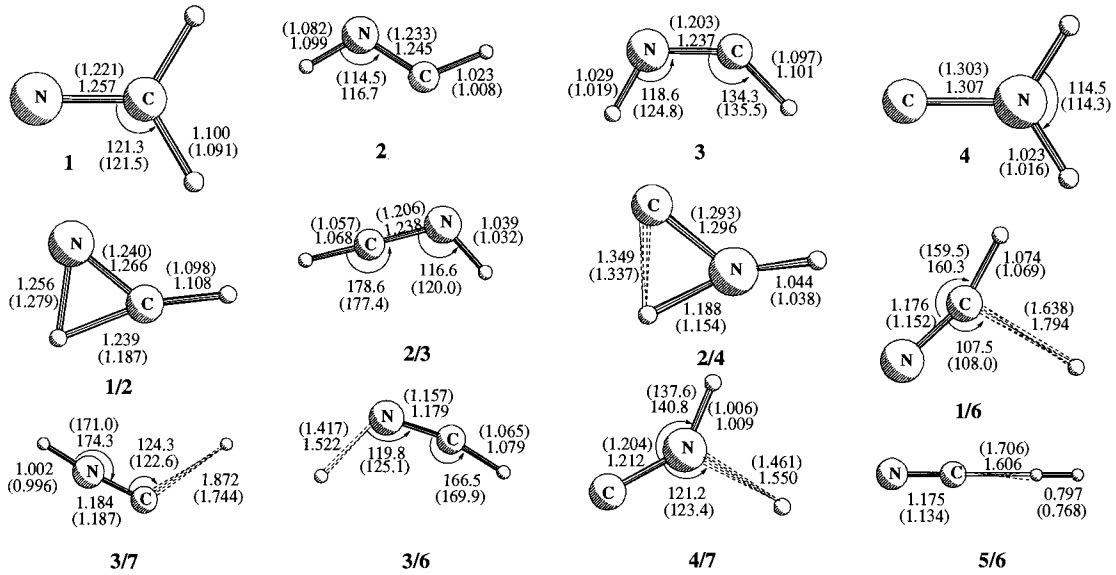

Figure 2. CCSD(T)/6-311++G(d,p) optimized geometries of the stationary points **1**, **2**, **3**, **4**, **1**/**2**, **2**/**3**, **2**/**4**, **1**/**6**, **3**/**6**, **3**/**7**, **4**/**7** on the doublet [CH_2N] energy surface.

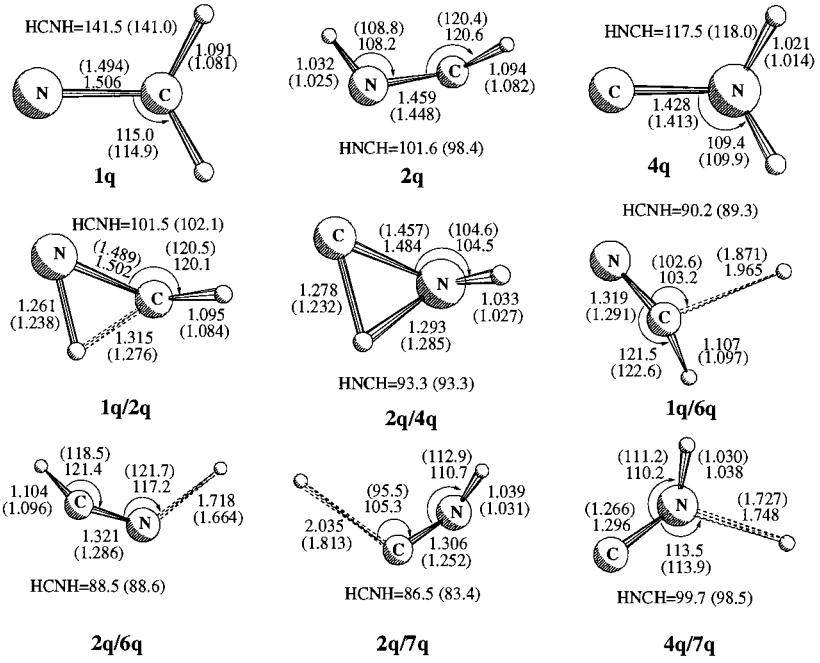

Figure 3. CCSD(T)/6-311++G(d,p) optimized geometries of the stationary points **1q**, **2q**, **4q**, **1q**/**2q**, **2q**/**4q**, **1q**/**6q**, **2q**/**6q**, **2q**/**7q**, **4q**/**7q** on the quartet [CH_2N] energy surface.

It is obvious from the doublet PES (Figure 1a) that the routes involving **2** → **4** isomerization could be excluded in the kinetics of H+HCN or H+HNC reaction due to the involvement of a rather high barrier for this conversion. Similarly, the endothermic hydrogen abstraction H+HCN, **6** → H_2 + CN, **5**, is less significant as compared with the HNC formation. The rate constant for this bimolecular reaction is obtained from the Arrhenius expression, $k = A \exp(-E_a/RT)$ where A is the frequency factor, E_a is the activation energy, and T is the temperature. The calculated direct hydrogen abstraction rate constant at 500 K and 1 atm is 36.3 $cm^3\ mol^{-1}\ s^{-1}$.

While the rate determining step in route A corresponds to **1** → **2** isomerization, in route C, the back dissociation into H+HCN is expected to be competitive with the product (H+HNC) formation. Most importantly, in all these routes, the initially formed energized adduct, either **1** or **3**, requires additional energy for its conversion into H+HNC. On the other hand, the reverse of route C suggests the existence of an energetically feasible channel for the conversion of HNC into HCN from the initially formed energised adduct **3**. Note that the unimolecular conversion HNC → HCN is associated with an energy barrier of about 30 kcal/mol, relative to HNC.[8] In this sense, the isonitrile−nitrile conversion will be greatly facilitated in the presence of the hydrogen atom.

Figure 2 shows that the calculated saddle point structure of the direct hydrogen abstraction reaction, H_2+CN, **5** → H+HCN, **6**, closely resembles the reactants. The C−N bond distance remains essentially a constant during the reaction signifying an early transition state in consistent with the Hammond's postulate for exothermic reactions. The calculated barrier for this process at the CCSD(T) level equals to 4.8 kcal/mol and is roughly 1.4 kcal/mol lower than that estimated by Bair and Dunning[13] using the POL-CI calculations. Wagner et al.[14] have theoretically computed the rate constant for this reaction using the conven-

tional transition state theory in conjunction with the PES reported by Bair et al.[13] and their computed rate constant was represented by the form $4.9 \times 10^{-18}\ T^{2.45}\ \exp(-1126/T)$ $cm^3\ mol^{-1}\ s^{-1}$ over the temperature range of 250−3500 K. The barrier heights employed for this channel in the earlier theoretical dynamic studies[7b] are 5.45, 4.2, and 5.2 kcal/mol. The ab initio calculations by ter Horst et al.[7a] using a multireference configuration interaction method with large correlation consistent basis sets yielded a barrier of about 4.3 kcal/mol for this hydrogen abstraction. It is thus clear that the state-of-the-art ab initio calculations at both single and multireference levels provide a barrier of about 4.5 ± 0.3 kcal/mol for this channel. However, the rate constant calculations by ter Horst et al. using the ab initio barrier height yielded a low rate constant value, and they, in fact, adjusted this barrier energy to 3.2 kcal/mol so as to get rate constants that are close to the experimental values.

On the quartet PES, both H_2CN, **1q**, and HCNH, **2q**, species have a nonplanar structure (cf. Figure 3, **q** stands for quartet). The barriers for the formation of the pyramidalized H_2CN, **1q**, as well as the nonplanar HCNH from the triplet HCN, **6q**, are low (2.8 and 3.7 kcal/mol, respectively) compared to those on the ground doublet energy surface. As can be seen from Figure 1b, **1q** could undergo 1,2-hydrogen shift spontaneously via **1q**/**2q** and redissociate back into H+HCN. The barrier for H+HNC formation from **2q** is 10.9 kcal/mol higher than that for the dissociation into H+HCN. Hence, on the quartet PES, isomerization of HCN to HNC is less favorable. Indeed, HNC would undergo assisted isomerization to HCN by the following pathways:

$$\mathrm{H + HNC} \quad \mathbf{7q \rightarrow 2q \rightarrow 1q} \rightarrow \mathrm{H + HCN} \quad \mathbf{6q}$$

$$\mathrm{H + HNC} \quad \mathbf{7q \rightarrow 4q \rightarrow 2q \rightarrow 1q} \rightarrow \mathrm{H + HCN} \quad \mathbf{6q}$$

In the triplet state, HNC remains less stable than HCN but with a slightly reduced energy difference, namely, 10 kcal/mol instead of 14.4 kcal/mol in the singlet state. The 1,2-H shift connecting both forms involves an energy barrier of 36.4 kcal/mol, relative to HNC($^3A''$), which is slightly larger than that of 30 kcal/mol in the singlet counterpart. Note also that the triplet HCN lies about 110.4 kcal/mol above singlet HCN but about 15 kcal/mol below the H + CN dissociation limit.

We now turn to the second part of this work which is a kinetic analysis of H+HCN and H+HNC reactions associated with the $[CH_2N]$ potential energy surface. Thus, the apparent rate constants of these reactions: (1) H+HCN (C-attack), (2) H+HCN (N-attack) (3) H+HNC (C-attack), and (4) H+HNC (N-attack) have been computed using QRRK model. We use the PES obtained at the CCSD(T)/6-311++G(3df,3pd)//CCSD-(T)/6-311++G(d,p) level and the vibrational frequencies and rotational constants calculated at the UMP2/6-31G(d,p) level as input parameters for the QRRK calculations. Recent publications[20−29] reveal that processes involving high energy chemically activated adducts with non-Boltzmann distribution can be characterized by the simple QRRK method with reasonable accuracy. The advantages and limitations of this approach over the more rigorous RRKM treatment are well outlined in ref 30. The kinetic treatment and the method of evaluation of the apparent rate constants for the stabilization of adducts and for the dissociation into products are well described in our previous papers[20−28] and molecular nitrogen has been used as a bath gas in the present study.

3.1. The H+HCN Reaction (Reactions 1 and 2). Due to the fact that the quartet PES lies well above the doublet (Figure 1), it is reasonable to consider the H+HCN reaction as happening only on the doublet PES. As discussed above, the H+HCN reaction can give rise to either H_2CN, **1**, or *cis*-HCNH, **3**, as the initially formed energized adduct, and hence the kinetics, of this reaction has been analysed by starting from both H_2CN (reaction 1) and *cis*-HCNH (reaction 2) potential wells. Because the rate constants for product formation depend highly on the internal energy of the adduct, the lifetimes of the intermediates and the coupling of vibrational coordinates to the reaction coordinate, the product distributions originating from these two additions are expected to be markedly different. For reaction 1, we define the apparent rate constants of the various channels in Figure 1 as follows Similarly, for reaction 2,

k_1^1: H + HCN → H_2CN **1**

k_2^1: H + HCN → *trans*-HCNH **2** via **1**

k_3^1: H + HCN → *cis*-HCNH **3** via **1** and **2**

k_4^1: H + HCN → CNH_2 **4** via **1**, **2**, and **3**

k_6^1: H + HCN → H+HCN **6** via **1**

$k_{7,3}^1$: H + HCN → H+HNC **7** (via route A; **1**, **2**, and **3**)

$k_{7,4}^1$: H + HCN → H+HNC **7** (via route B; **1**, **2**, and **4**)

k_1^2: H + HCN → H_2CN **1** (via **3** and **2**)

k_2^2: H + HCN → *trans*-HCNH **2** (via **2**)

k_3^2: H + HCN → *cis*-HCNH **3**

k_4^2: H + HCN → CNH_2 **4** (via **2**)

k_6^2: H + HCN → H+HCN **6** (via **3**, **2**, and **1**)

$k_{7,3}^2$: H + HCN → H+HNC **7** (via route C; **3**)

$k_{7,4}^2$: H + HCN → H+HNC **7** (via route D; **3**, **2**, and **4**)

The superscript and subscript in the rate constant definitions correspond, respectively, to the reaction number and the product number as shown in Figure 1a. The calculated apparent rate constants k_2^1, k_3^1, and k_4^1 were found to be very low and hence are not shown in figures. The total rate constant k_T^1 for the disappearance of the H+HCN reactants was calculated as the sum of all apparent rate constants, except for k_6^1 and k_6^2, because these channels regenerate back the reactants. Figure 4 shows the variation of the apparent rate constants as a function of pressure at 300 K. The predominant contribution to the total rate constant k_T^1 comes from the stabilization of the initially formed H_2CN adduct k_1^1. The total rate constant and, hence k_1^1, becomes pressure independent at atmospheric pressure. Because the barrier for the isomerization of **1** → **2** is higher than the entrance channel barrier, redissociation back to H+HCN is the only favored route available to **1** at ordinary temperatures and pressures. This, in turn, explains the low magnitude of the calculated k_2^1, k_3^1, and k_4^1 rate constants. The total rate constant

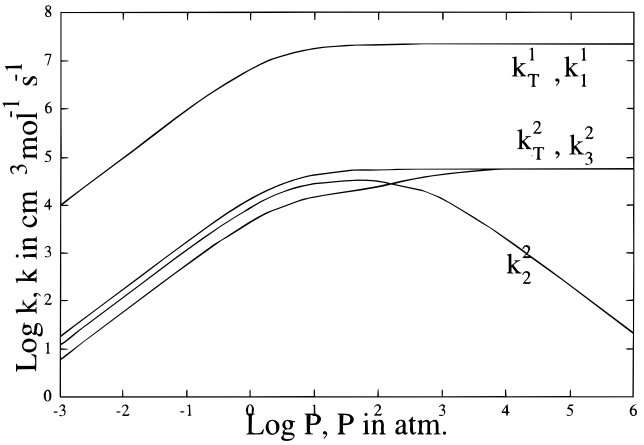

Figure 4. Plots of log apparent rate constants and total rate constant of H+HCN reaction versus log pressure.

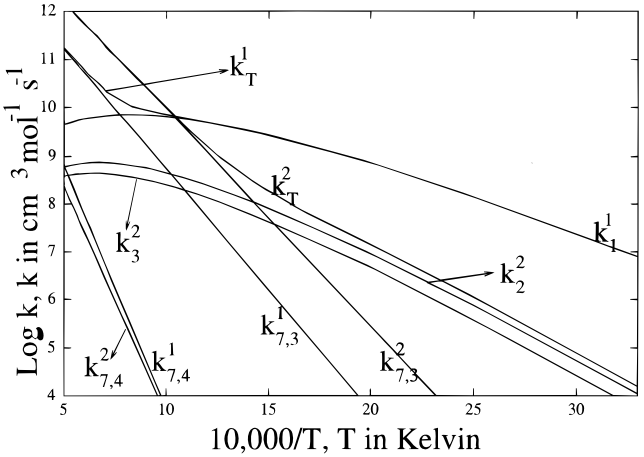

Figure 5. Plots of log apparent rate constants and total rate constant of H+HCN reaction versus $10^4/T$ (K) at 1 atm.

for reaction 2 is lower than that for reaction 1 due to the larger magnitude of the entrance channel barrier. In reaction 2, the initially formed *cis*-HCNH **3** could undergo spontaneous isomerisation to *trans*-HCNH **2**. However, the transition state for the H+HNC product formation is disposed energetically above the entrance channel barrier. Hence, the predominant contribution to k_T^2 comes from the stabilization rate constants k_3^2 and k_2^2. In the high-pressure region, while k_3^2 reaches a limiting value, k_2^2 decreases after passing through a maximum. This is due to the fact that at lower pressures (**3** → **2**) isomerization is appreciable even though the main channel is stabilization of **3**. Hence, at ordinary temperatures, H+HCN reaction is expected to lead to the formation of adducts. Our calculated k_∞ value at 300 K is 2.2×10^7 cm^3 mol^{-1} s^{-1}.

Figure 5 shows the variation of the apparent rate constants for the formation of the adducts and HNC product with temperature at atmospheric pressure. At all pressures, the H+HNC channel opens up only at higher temperatures. This is due to the fact that at lower temperatures the number of CH_2N **1** molecules formed with energy greater than or equal to the energy of **1**/**2** is small. Consequently, at lower temperatures, stabilization of the adduct **1** becomes the primary channel for the disappearance of the reactants. At low pressures, most of the initially activated CH_2N, **1**, once formed will redissociate to H+HCN. Increasing the pressure to a very high value leads to the stabilization of almost all the H_2CN, **1**, or c-HCNH, **3**. Hence, in the presence of hydrogen, relatively high temperatures are needed for the conversion of HCN to HNC. The isolated HCN molecule requires an energy of about 47.5 kcal/mol for its isomerization into HNC. Consequently, in the presence of hydrogen, although addition of hydrogen to the C≡N multiple bond is preferred, isomerization of HCN to HNC becomes somewhat accelerated.

3.2. The H+HNC Reaction (Reactions 3 and 4). The approach of H to HNC can also give rise to either *cis*-HCNH, **3**, or CNH_2 , **4**, as the initially formed energized adduct, and hence the kinetics of this reaction, has been analysed by starting from both *cis*-HCNH (reaction 3) and CNH_2 (reaction 4) potential wells. The several product channels which are energetically possible include H+HCN, **6**; *cis*-HCNH, **3**; *trans*-HCNH, **2**; H_2CN, **1**; CNH_2, **4**, as well as the reformation of H+HNC, **7**, via CNH_2, *trans*-HCNH, and *cis*-HCNH. We were not able to locate any transition structure for hydrogen abstraction converting H+HNC to H_2 + NC. In addition, no stable complex H−H···N≡C with a linear configuration could be found. We use the same PES for our kinetic analysis.

A glance at the PES (Figure 1a) reveals that when the more stable *cis*-HCNH **3** is formed initially, it undergoes at low pressures a preferential dissociation to H+HCN due to its low barrier height. For the reaction 3, we define the apparent rate constants as follows:

k_1^3: H+HNC → H_2CN **1** (via **3** and **2**)

k_2^3: H+HNC → t-HCNH **2** (via **3**)

k_3^3: H+HNC → c-HCNH **3**

k_4^3: H+HNC → CNH_2 **4** (via **3**, **2**, and **4**)

$k_{6,3}^3$: H+HNC → H+HCN **6** (via **3**)

$k_{6,1}^3$: H+HNC → H+HCN **6** (via **3**, **2**, and **1**)

k_7^3: H+HNC → H+HNC **7** (via **3**, **2**, and **4**)

Similarly for reaction 4, the different apparent rate constant definitions are as follows:

k_1^4: H+HNC → H_2CN **1** (via **4**, **2**, and **1**)

k_2^4: H+HNC → t-HCNH **2** (via **4**)

k_3^4: H+HNC → c-HCNH **3** (via **4** and **2**)

k_4^4: H+HNC → CNH_2 **4**

$k_{6,1}^4$: H+HNC → H+HCN **6** (via **4**, **2**, and **1**)

$k_{6,3}^4$: H+HNC → H+HCN **6** (via **4**, **2**, and **3**)

k_7^4: H+HNC → H+HNC **7** (via **4**, **2**, and **3**)

Figure 6 shows the variation of the apparent rate constants as a function of pressure at 300 K. The predominant contribution to the total rate constant comes exclusively from $k_{6,3}^3$ except at very high pressures where the stabilization of *cis*-HCNH, **3**, outruns their dissociation to H+HCN. In the lower pressure region, both k_3^3 and k_2^3 increase with increasing pressures. In the high pressure region, while k_3^3 reaches a limiting value, k_2^3 and k_1^3 decrease after passing through a maximum. This is due to the fact that, at lower pressures, **3** → **2** → **1** isomerization is appreciable even though the important

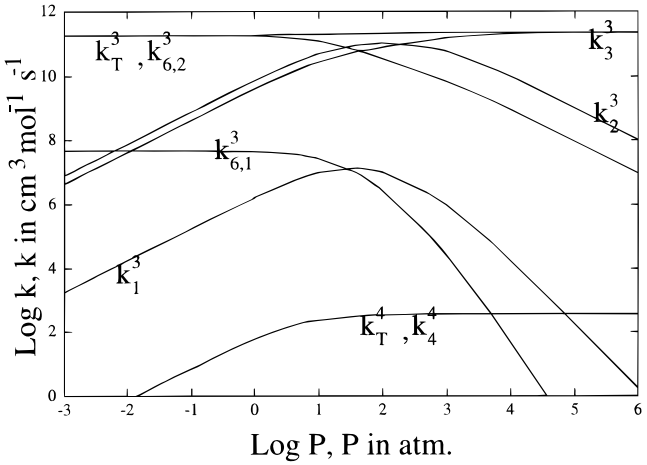

Figure 6. Plots of log apparent rate constants and total rate constant of H+HNC reaction versus log pressure at 300 K.

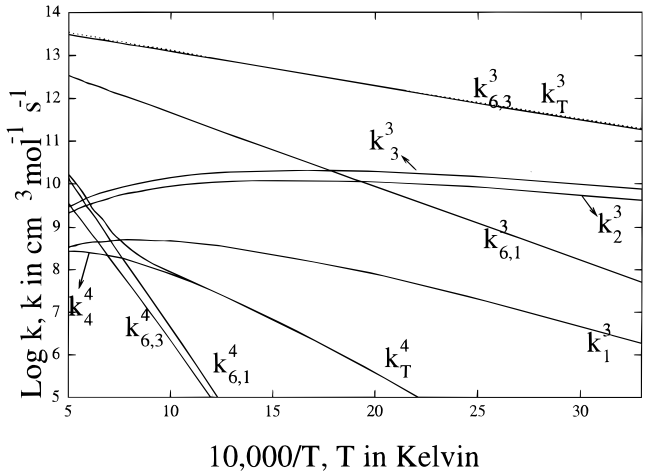

Figure 7. Plots of log apparent rate constants and total rate constant of H+HNC reaction versus $10^4/T$ (K) at 1 atm.

channel is **3** → H+HCN, **6**. At very high pressures, stabilization of **3** takes place at the cost of **3** → **2** isomerization. Also, as is evident from Figure 6, that the pressure independent total rate constant of reaction 4 at 300 K is roughly 9 orders of magnitude lower than that of reaction 3 and this is essentially due to the large magnitude of the entrance channel barrier for the former reaction. Thus, it suggests that the addition of hydrogen would occur preferentially at the carbon end of HNC.

Figure 7 displays the variations of all the apparent rate constants for reactions 3 and 4 with temperature at atmospheric pressure. At all temperatures, formation of H+HCN, **6**, is found to be the predominant channel. The rate constant for H+HCN formation in reaction 3 is much higher than that in reaction 4 at all temperatures and pressures due to the large magnitude of the entrance channel barrier for reaction 4. Stabilization of CNH_2, **4**, adduct (k_4^4) contributes predominantly to the total rate constant of reaction 4. This is due to the fact that the barrier for the conversion of **4** to **2** is higher than the entrance channel barrier. The calculated total apparent rate constant for the H+HNC reaction at 300 K is 1.85×10^{11} cm^3 mol^{-1} s^{-1}.

3.3. Heat of Formation of H_2CN. We take this opportunity to have a brief comment on the heat of formation of the radical H_2CN, **1**, which, as far as we are aware, is not well established yet. On the basis of the measured electron affinity for **1** (EA-(H_2CN) = 11.8 kcal/mol), Cowles et al.[31] derived a value $\Delta H^0_{f,298}$ (H_2CN) = 60 ± 6 kcal/mol and the heat of formation of methanimine, $\Delta H^0_{f,298}$ (H_2CNH) = 26 kcal/mol. Shortly afterward, the latter value has been reevaluated to a considerably lower value,[32] $\Delta H^0_{f,298}$ (H_2CNH) = 16.5 kcal/mol. This new value led Cowles et al.[31] to propose a corrected value $\Delta H^0_{f,298}$ (H_2CN) = 51 ± 6 kcal/mol. The latter has been utilized in evaluating the ionization energy of H_2CN.[33]

Nevertheless, the heat of formation of methanimine remains apparently a matter of discussion. In fact, two new values have recently been reported; the first value was derived from ab initio calculations.[34] Upon evaluation to check the consistency with available thermochemical data,[35,36] the value of 21 ± 2 kcal/mol has been suggested. The most recent evaluation[37] using a thermokinetic method and based on the gas phase proton transfer reactions yielded a lower value of 17.9 ± 1 kcal/mol. It seems that the earlier values of 26 and 16.5 kcal/mol constitute the upper and lower limits, respectively, for the heat of formation of $H_2C{=}NH$. As a consequence, the standard heat of formation of the H_2CN radical lie well in the range of 60 and 51 kcal/mol.[31] Combination of energy differences obtained from CCSD-(T) calculations in the present work (Figure 1) with literature data,[33] gives values close to the upper limit, namely, 56−57 kcal/mol (value at 298 K; the corresponding 0 K value being 57−58 kcal/mol). Earlier calculations[13,33] also sugested values in the range of 55−59 kcal/mol. It is obvious that further experimental and theoretical studies are still needed to achieve a consistent set of thermochemical parameters for [CH_nN] species attaining the chemical accuracy. Some other useful parameters calculated for H_2CN involve its moment of inertia (6.2, 44.5, and 50.7 au) and C_v (6.7 cal/mol K). The corresponding parameters for the experimentally less studied HNC are 40.7 au and 7.5 cal/mol K, respectively.

4. Concluding Remarks

Both electronic structure and rate theory calculations have been used to probe the reactions occuring on the lowest doublet PES of [CH_2N] system. The quartet PES has also been constructed. Geometries for stationary points on the PES are determined with the CCSD(T)/6-311++G(d,p) level of theory. With the use of these geometries, relative energies are determined with CCSD(T)/6-311++G(3df,3pd) calculations.

Direct hydrogen abstraction reaction is confirmed to be the main channel of the H_2 + CN process. The addition intermediates on the doublet potential energy surface are H_2CN, **1**, *trans*-HCNH, **2**, *cis*-HCNH, **3**, and CNH_2, **4**. The competitive product channels are H+HCN and H+HNC. For its part, the H+HCN reaction leads to the stabilisation of the adducts at ordinary temperatures and pressure while the H+HNC reaction leads to the isomerization/dissociation product, H+HCN. Our calculated total rate constants amount to 2.2×10^7 cm^3 mol^{-1} s^{-1} for H+HCN and 1.81×10^{11} cm^3 mol^{-1} s^{-1} for H+HNC; there exists no experimental value for comparison. On the quartet surface, H+HCN reaction would again lead to the stabilisation of the adducts and at lower pressures predominantly a redissociation back to H+HCN. The heat of formation of the H_2-CN radical is estimated to be 56 kcal/mol at 298 K and 57 kcal/mol at 0 K, with an error of, at most, ±3 kcal/mol.

Acknowledgment. We are indebted to the Fund for Scientific Research (FWO-Vlaanderen) and Geconcerteerde Onderzoeksakties (GOA) for financial support and to the KU Leuven Computer center for providing computer facilities.

Supporting Information Available: Tables of unscaled UMP2/6-31G(d,p) harmonic vibrational frequencies of the

minima and saddle points in the doublet and quartet H_2CN PES (2 pages). Ordering information is given on any current masthead page.

References and Notes

(1) Miller, J. A.; Bowman, C. T. *Prog. Energy Combust Sci.* **1989**, *15*, 287.

(2) Melius, C. F. In Chemistry and Physics of Energetic Materials; NATO ASI Series; Bulusu, S. N., Ed.; Kluwer Academic Publishing: Dordrecht, Netherlands, 1990; p 51.

(3) (a) Szekely, A.; Hanson, R. K.; Bowman, C. T. *Int. J. Chem. Kinet.* **1983**, *15*, 915. (b) Wooldridge, S. T.; Hanson, R. K.; Bowman, C. T. *Int. J. Chem. Kinet.* **1996**, *28*, 243.

(4) Albers, E. A.; Hoyermann, K.; Shacke, H.; Schmatjko, K. J.; Wagner, H. G.; Wolfrum, J. *Proceedings of the 15th International Symposium on Combusion*; The Combustion Institute: Pittsburgh, 1984.

(5) Boden, J. C.; Thrush, B. A. *Proc. R. Soc. London, Ser. A* **1968**, *305*, 107.

(6) (a) Li, X.; Sayah, N.; Jackson, W. M. *J. Chem. Phys.* **1984**, *81*, 833. Schacke, H.; Wagner, H. Gg.; Wolfrum, J. *Ber. Bunsen-Ges Phys. Chem.* **1977**, *81*, 670.

(7) (a) ter Horst, M. A.; Schatz, G. C.; Harding, L. B. *J. Chem. Phys.* **1996**, *105*, 558. (b) Brooks, A. N.; Clary, D. C. *J. Chem. Phys.* **1990**, *92*, 4178. (c) Clary, D. C. *J. Phys. Chem.* **1995**, *99*, 13664.

(8) (a) Nguyen, M. T.; Groarke, P. G.; Malone, S.; Hegarty, A. F. *J. Chem. Soc., Perkin Trans. 2* **1994**, 807. (b) Lee, T. J.; Rendell, A. P. *Chem. Phys. Lett.* **1991**, *177*, 491. Bentley, J. A.; Bowman, J. M.; Gazdy, B.; Lee, T. J.; Dateo, C. E. *Chem. Phys. Lett.* **1992**, *198*, 563. Bowman, J. M.; Gazdy, B.; Bentley, J. A.; Lee, T. J.; Dateo, C. E. *J. Chem. Phys.* **1993**, *99*, 308. (c) Thomas, J. R.; DeLeeuw, B. J.; Vacek, G.; Crawford, T. D.; Yamaguchi, Y.; Schaefer, H. F., III *J. Chem. Phys.* **1993**, *99*, 403.

(9) Lin, M. C.; He, Y.; Melius, C. F. *Int. J. Chem. Kinet.* **1992**, *24*, 489.

(10) Goldsmith, P. F.; Langer, W. D.; Ellder, J.; Irvine, W.; Kollberg, E. *Astrophys. J.* **1981**, *249*, 521.

(11) Jentz, D.; Trenary, M.; Peng, X. D.; Stair, P. *Surf. Sci.* **1995**, *341*, 282.

(12) Chipman, D. M.; Carmichael, I.; Feller, D. *J. Phys. Chem.* **1992**, *95*, 4702.

(13) Bair, R. A.; Dunning, T. H., Jr. *J. Chem. Phys.* **1985**, *82*, 2280.

(14) Wagner, A. F.; Bair, R. A. *Int. J. Chem. Kinet.* **1986**, *18*, 473.

(15) Nguyen, M. T.; Sengupta, D.; Ha, T. K. *J. Phys. Chem.* **1996**, *100*, 6499.

(16) Peeters, J.; Nguyen, M. T. 1998. Unpublished Results.

(17) Dean, A. M. *J. Phys. Chem.* **1985**, *89*, 4600.

(18) Frisch, M. J.; Trucks, G. W.; Gordon, M. H.; Gill, P. M. W.; Wong, M. W.; Foresman, J. B.; Johnson, B. G.; Schlegel, H. B.; Robb, M. A.; Replogle, E. S.; Gomperts, R.; Andres, J. L.; Raghavachari, K.; Binkley, J. S.; Gonzalez, C.; Martin, R. J.; Fox, D. J.; Defrees, B. J.; Baker, J.; Stewart, J. J. P.; Pople, J. A. *Gaussian 94*, Gaussian, Inc.: Pittsburgh, PA, 1994.

(19) Nguyen, M. T.; Hegarty, A. F.; Sana, M.; Leroy, G. *J. Am. Chem. Soc.* **1985**, *107*, 4141.

(20) Sengupta, D.; Chandra, A. K. *J. Chem. Phys.* **1994**, *101*, 3906.

(21) Nguyen, M. T.; Sengupta, D.; Vanquickenborne, L. G. *Chem. Phys. Lett.* **1995**, *240*, 513.

(22) Nguyen, M. T.; Sengupta, D.; Raspoet, G.; Vanquickenborne, L. G. *J. Phys. Chem.* **1995**, *99*, 11883.

(23) Nguyen, M. T.; Sengupta, D.; Verecken, L.; Peeters, J.; Vanquickenborne, L. G. *J. Phys. Chem.* **1996**, *100*, 1615.

(24) Nguyen, M. T.; Sengupta, D.; Vanquickenborne, L. G. *J. Phys. Chem.* **1996**, *100*, 10956.

(25) Sengupta, D.; Nguyen, M. T. *Mol. Phys.* **1996**, *89*, 1567.

(26) Sengupta, D.; Nguyen, M. T. *Chem. Phys. Lett.* **1997**, *265*, 35.

(27) Sumathi, R.; Peyerimhoff, S. D. *Chem. Phys. Lett.* **1996**, *263*, 742.

(28) Sumathi, R.; Peyerimhoff, S. D. *J. Chem. Phys.* **1998**. (In press).

(29) Dean, A. M.; Westmoreland, P. R. *Int. J. Chem. Kinet.* **1987**, *19*, 207.

(30) Weston, R. E. *Int. J. Chem. Kinet.* **1986**, *18*, 1259.

(31) Cowles, D. C.; Travers, M. J.; Frueh, J. Y.; Ellison, G. B. *J. Chem. Phys.* **1991**, *94*, 3517.

(32) Peerboom, R. A. L.; Ingemann, S.; Nibbering, N. M. M.; Liebman, J. F. *J. Chem. Soc., Perkin Trans. 2* **1990**, 1825.

(33) Nesbitt, F. L.; Marston, G.; Stief, L. J.; Wickramaaratchi, M. A.; Tao, W.; Klemm, R. B. *J. Phys. Chem.* **1991**, *95*, 7613.

(34) Smith, B. J.; Pople, J. A.; Curtius, L. A.; Radom, L. *Aust. J. Chem.* **1992**, *45*, 285.

(35) Holmes, J. L.; Lossing, F. P.; Mayer, P. M. *Chem. Phys. Lett.* **1992**, *198*, 211.

(36) Nguyen, M. T.; Rademakers, J.; Martin, J. M. L. *Chem. Phys. Lett.* **1994**, *221*, 149.

(37) Bouchoux, G.; Salpin, J. Y. *J. Phys. Chem.* **1996**, *100*, 16555.